ACS Macro Letters
Letter
pubs.acs.org/macroletters

Packed Colloidal Phases Mediate the Synthesis of Raspberry-Structured Microgel Heteroaggregates

Jeffrey C. Gaulding,[†] Shalini Saxena,[‡] Danielle E. Montanari,[†] and L. Andrew Lyon*,[†]

[†]School of Chemistry and Biochemistry and the Petit Institute for Bioengineering & Bioscience, and [‡]School of Materials Science and Engineering, Georgia Institute of Technology, Atlanta, Georgia 30332, United States

Supporting Information

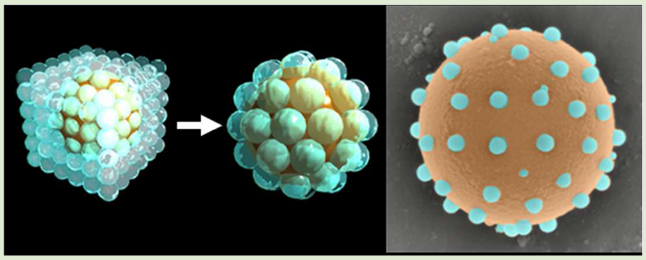

ABSTRACT: Hybrid nanoparticles with complex architectures combine the properties of two distinct materials and integrate them to synergistically provide new characteristics to the assembly. In this work we demonstrate the ability to decorate the surface of a variety of micrometer-sized "core" particles with responsive microgels, forming raspberry-like particles. We use a templating technique wherein the microgel coating is applied from a high-volume-fraction colloidal phase, leading to high surface coverage and enhanced colloidal stability of the resultant particles. Concentrated colloidal dispersions enable microgel/core combinations driven by both specific and nonspecific interactions and offer improved coverage relative to dilute heteroaggregation. This approach is versatile and allows both the core material and microgel phase to be altered while still remaining effective. Though the recovered particles are highly diluted, recycling the unincorporated microgels following raspberry-like particle isolation and reforming the packed colloidal assembly allow multiple cycles of particle synthesis, which improves overall yield.

Architectural control of nano- and microparticles is a powerful method for modulating the properties of colloidal materials.[1] In particular, hybrid colloids wherein two distinct materials form a core−shell architecture are enabling for applications such as drug delivery[2] and catalysis.[3] One common and versatile approach is the utilization of templates for directed assembly of heterogeneous materials, especially in the case where the surface layer itself consists of nanoparticles. Self-assembly via ion pairing has been extensively demonstrated for the formation of nanoparticle heteroaggregates,[4] where solution conditions have a strong impact on the surface coverage.[5] Hydrogen bonding or other types of complementary interactions have also been utilized.[6] The resultant particles consist of a shell of nanoparticles decorating the template "core", leading to a bumpy surface reminiscent of raspberries. The anisotropy and tunability in surface roughness have made particles of this nature useful in altering the hydrophobicity of surfaces, for example.[7]

In the work described herein, we utilize hydrogel particles (microgels) in the fabrication of hybrid colloids. Microgels are of great interest due to their applicability to a variety of fields such as sensing and drug delivery.[8] In particular, thermoresponsive microgels composed of poly(*N*-isopropylacrylamide) (pNIPAm) have been extensively studied either as homopolymers[9] or as copolymers with other environmentally sensitive monomers (e.g., acidic and basic monomers) to produce materials responsive to multiple stimuli.[10] The responsivity of microgels has been exploited in Coulombically directed heteroaggregation to form hybrid raspberry-like particles (RLPs),[11] and similar particles have been formed that utilize microgels as templates for colloidal shell addition.[12] In addition, thin films of microgels coated onto solid substrates have been shown to improve the biocompatibility of the base material[13] and allow controlled drug release from that surface.[14] As such, microgels are an attractive material for incorporation into hybrid constructs for controlled delivery, wherein the assembly of microgels on core particles would confer soft, responsive properties to the core particle while providing an opportunity for a multicompartment or multifunctional vehicle. Additionally, microgels have been shown to exhibit rich phase behavior as concentrated dispersions due to their high water content and responsive nature.[15] In this work, we exploit the soft, responsive matrix provided by packed colloidal phases of microgels (e.g., colloidal glasses or crystals) to generate hybrid particles whose surfaces are decorated with hydrogel colloids. Our method is outlined in Scheme 1.

By introducing a variety of "core" particles to act as templates in a concentrated colloidal phase, the surfaces become decorated with a close-packed monolayer of microgels. The high volume fraction and close packing of the colloidal phase enable this method to generate decorated particles in the absence of complementary surface chemistries, which ordinarily drive heteroaggregation in dilute media. Due to the amphiphilic nature and chemical versatility of these microgels, the resultant RLPs can be stabilized on a variety of functional core particle

Received: December 11, 2012
Accepted: April 2, 2013
Published: April 5, 2013

Scheme 1. Raspberry-Like Particle Synthesis

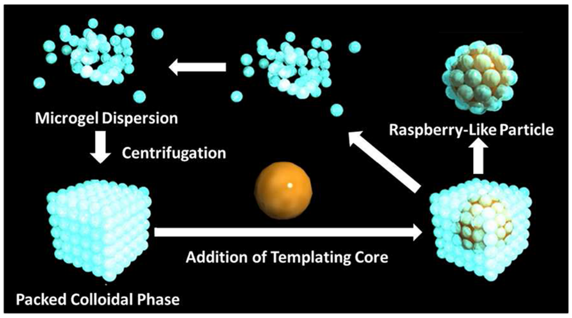

surfaces. Upon dispersion of the colloidal phase, the remaining microgels are then easily recovered and recycled to re-form another packed colloidal phase for RLP synthesis.

A number of "core" particles are available commercially, permitting the exploration of different surface chemistries, size ratios, and surface structures. The microgel compositions investigated are outlined in Table 1. We found that concentrating the microgels into a concentrated colloidal phase (a colloidal fluid or glass from a spatial point of view) prior to introduction of the core particles led to the coordination of the core particles' surfaces with a large number of microgels, ensuring high surface coverage. Additionally, this coordination leads to assembly in the absence of complementary surface interactions. The high viscosity of the dense colloidal phase tends to stabilize the cores against aggregation, which can be a problem in dilute solutions when assembling multiple multivalent building blocks via heteroaggregation.

Highly packed microgel assemblies were prepared by centrifugal sedimentation, as described previously.[16] Under applied centrifugal forces, sedimentation serves to concentrate the microgels into a fraction of the available volume, until close-packing of the colloidal particles leads to pellet formation. Removal of the supernatant confines the volume available for the microgels to redisperse, thus the remnant microgels are trapped in a highly concentrated glassy state. In all cases, the resultant pellet was viscous and turbid and appeared homogeneous with no evidence of Bragg diffraction, as is consistent with disordered packed phases prepared by our group in previous studies.[15a] Core particles were then introduced to the colloidal phase and incorporated within the matrix via vortexing. As shown in Figure 1, the core particles are distributed throughout the microgel colloidal phase. Following incubation of the cores within the matrix for 30 min, isolation of stable RLPs followed dilution of the colloidal assembly. The much greater density of the core particles and subsequent RLPs led to facile isolation of the RLPs from the excess unincorporated microgels via sedimentation. The excess microgels could then be recovered and returned to a colloidal packed state for sequential rounds of RLP assembly.

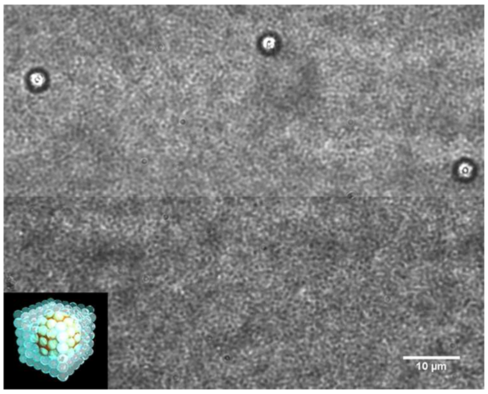

Figure 1. Bright-field microscopy image of aminobenzophenone-functionalized 4.6 μm diameter magnetic polystyrene particles mixed in a dense colloidal phase of μgel-G.

Upon isolation, the relative scattering intensity of the core particles and the microgels made bright-field visualization of the adsorbed microgels impossible. However, by incorporating a fluorescent monomer within the microgel network, the labeled particles are observed to colocalize with the cores, as shown in Figure 2, and discrimination of individual microgels is possible.

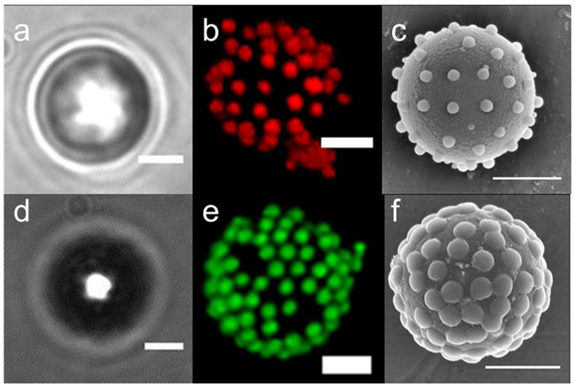

Figure 2. (a,d) Bright-field, (b) green-excitation, or (e) blue-excitation confocal, microscopy, and (c,f) scanning electron microscopy (SEM) images of isolated RLPs. (a−c) 4.4 μm AB-functionalized PS decorated with μgel-R. (d−f) 4.6 μm AB-functionalized magnetic PS decorated with μgel-G. The scale bar in each image is 2 μm.

Once the core particles have become mixed within the high volume fraction colloidal phase, a variety of specific and nonspecific interactions, discussed in the Supporting Information, may lend stability to the resultant RLPs. Shown in Figure 2 are carboxylated polystyrene (PS) core particles conjugated to 4-aminobenzophenone (AB) decorated with microgels. Under UV excitation, AB forms covalent linkages with numerous organic groups, including simple aliphatic C−H bonds via hydrogen abstraction.[17] We have previously demonstrated this technique to conjugate microgels to functionalized polyethylene terephthalate surfaces.[18] As such, AB-bearing core particles would be expected to covalently bind decorated microgels regardless of the microgel functionality. Importantly, the use of the packed colloidal phase-mediated

Table 1. Microgel Compositions and Characterization

	mol % NIPAm	mol % BIS	mol % AAc	R_H (pH 3), nm[a]	R_H (pH 5.5), nm[a]	zeta potential (pH 5.5), mV	radius on surface, nm[b]
μgel-R	70.5	3.5	26	366	553	−23.0	475
μgel-G	96.0	4.0	0	437	448	−1.4	650

[a] Measured by dynamic light scattering at 20 °C and 15 mM ionic strength. [b] Estimated from atomic force microscopy (AFM) line traces.

technique showed improved surface coverage relative to stoichiometrically matched controls performed under relatively dilute conditions (see Supporting Information).

Quantifying or predicting the effective coverage of each particle is challenging. To estimate the number of microgels per core particle, one must consider the total surface area of a single core particle and the contact area of the microgels. However, the soft nature of the microgels makes the latter point nontrivial to determine. Two limiting cases can be envisioned—one wherein the microgels are treated as hard spheres and thus exhibit minimal spreading upon contact with the core surface. In this case, the number of particles per core would be maximized, as the relative footprint of each microgel will be at a minimum and thus a greater number can be packed onto the surface of the spherical core. The other extreme assumes highly deformable particles, wherein the microgels spread on the surface. Approximating these adsorbed microgels as hemispheres, the number of particles on the surface will always be less than that of the hard-sphere case. The range of particle number densities captured by the two models varies according to the ratio of the radii of the microgels and the core particles, becoming highly sensitive to the spreading assumption when the cores and microgels are similar in size. Additional discussion of these cases is available in the Supporting Information.

For the case of the RLPs shown in Figure 2c, the average radius of μgel-R is approximately 550 nm, and the average PS core radius is approximately 2.2 μm. This leads to a surface coverage of between 54 and 84 microgels per particle. Though quantitative measurement of the number of microgels on the surface is challenging using microscopic techniques, semi-quantitative assessment of the SEM image in Figure 2c indicates that this is a reasonable approximation. Figure 2 also provides some insight into the microgel/surface interaction. Visualization of swollen microgels, as in Figure 2b and 2e, seems to indicate that the microgels are densely packed on the surface, as we expect from the templating colloidal phase. Thus, for μgel-R comparison of Figure 2b and 2c suggests that upon vacuum drying the particles deswell isotropically, leading to a reduction in apparent dry particle diameter to approximately 30% of that observed via AFM. This suggests that the effective particle footprint is commensurate with that of a spherical microgel contacting a spherical core. Deformation upon contacting the core surface and the resultant spreading would lead to surface pinning of the spread state and more anisotropic deswelling of the microgels, as is typically seen via AFM. This isotropic deswelling in all dimensions save the points anchored to the core substrate underneath contributes to the apparent sparseness of the surface coverage. In contrast, the neutral microgels (μgel-G) in Figure 2d−f appear to coat the surface in a more uniform manner and undergo more spreading with a reduction in particle diameter of approximately 50% of that observed via AFM. Greater microgel−microgel interactions may also be occurring in this case as well, as the particles appear to have more irregular spacing following deswelling and drying, though this may simply be more prominent due to the smaller discrepancy with respect to the AFM diameter.

The nature of the core particles can be used to impart additional functionality into the RLPs, such as paramagnetism. We chose rough-surface magnetic PS nanoparticles as a particularly challenging core. These particles were smaller (2.5 μm in diameter) than the cores described previously and had a very rough surface due to the presence of surface-grown polymer brushes containing adsorbed iron oxide nanoparticles (Figure 3a). However, these rough surface core particles were readily incorporated within the microgel colloidal phase, leading to successful RLP synthesis and recovery (Figure 3). This exemplifies one of the advantages of hybrid, compartmentalized vehicles such as these particles. The magnetic functionality of the core particles is conferred upon the entire assembly, while the soft and responsive nature of microgels dominates the surface interactions. Thus, the core material and the microgel coating retain different functionalities and synergistically benefit from the RLP assembly. Also notable in Figure 3c and 3e is that the characteristic surface deformations of μgel-G and μgel-R are preserved on a surface with both greater curvature and greater surface roughness.

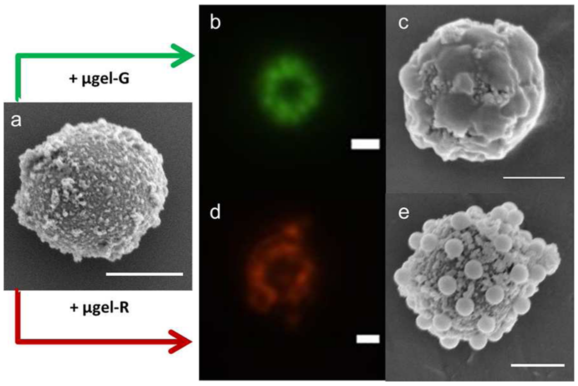

Figure 3. (a) SEM image of an AB-functionalized magnetic PS particle with rough surface topology. (b) Blue-excitation epifluorescence and (c) SEM image following coverage with μgel-G. (d) Green-excitation epifluorescence and (e) SEM image following coverage with μgel-R. Scale bar in all images is 1 μm.

In addition to high surface coverage and the stabilization of the core particles brought about by the high microgel packing densities, another advantage that arises from the use of jammed microgel phases is the ability to make multifunctional raspberry-like coatings, or patchy particles. Microgel colloidal crystals have been shown to be highly defect-tolerant,[15b] which enables mixtures of compositionally distinct microgels in a single colloidal phase without extensive phase segregation. Thus we reasoned that multiple distinct microgels should be able to form a mixed coating on the surface of the core. We demonstrated this using μgel-R and μgel-G. The two particles when sufficiently mixed in the glassy state by vortexing yielded a homogeneously colored pellet. Upon introduction of the AB-functionalized core particles, followed by UV excitation, RLPs were recovered with both types of microgels present on their surface, as shown in Figure 4. Comparison of the microgel morphologies via SEM in Figure 4 to their respective panels in Figure 2 shows the characteristic differences in surface spreading between the two microgels.

Though this method shows a great deal of versatility, especially with regard to the absence of the necessity for complementary interactions, there are several practical limitations. The inefficiency of microgel incorporation due to the large excess of particles inherent in the technique is only somewhat ameliorated by the ability to recycle the residual microgels. While the ratio of cores to microgels within the matrix has a theoretical maximum based on monolayer coverage of microgels, the practical limit for incorporation

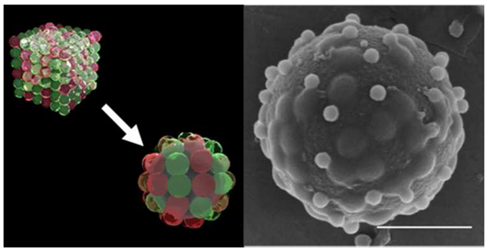

Figure 4. (Left) Schematic of mixed colloidal glass for raspberry coating. (Right) SEM image of 4.4 μm diameter AB-functionalized PS particles decorated with a 1:1 w:w mixture of μgel-R and μgel-G. Scale bar is 2 μm.

will be lessened by factors such as the core-addition solution and core mixing within the concentrated colloidal phase.

In summary, we have demonstrated that responsive microgels can be used to coat the surface of a variety of spherical, micrometer-scale substrates using a packed colloidal phase-mediated approach. The use of a high-volume fraction and high-viscosity phase during assembly provides a means to enable efficient surface coverage in the absence of compatible surface chemistries to direct such assembly from dilute media. This method seems highly tolerant with regard to microgel size, composition, and core substrate size, functionality, and topography. Mixtures of compositionally dissimilar microgels were also shown to form multifunctional surfaces. Overall, this method is a versatile technique that exploits the softness of responsive microgels to form densely packed assemblies on the surfaces of micrometer-scale particles, providing a flexible method to generate hybrid microgel constructs enabling drug delivery or other applications.

■ ASSOCIATED CONTENT

Ⓢ Supporting Information

Experimental methods, additional microgel characterization, core functionalities, and discussion of spreading and surface coverage. This material is available free of charge via the Internet at http://pubs.acs.org.

■ AUTHOR INFORMATION

Corresponding Author

*E-mail: lyon@gatech.edu.

Notes

The authors declare no competing financial interest.

■ ACKNOWLEDGMENTS

Funding for JCG was provided by the NIH (1 R01 GM088291-01) and the training grant: G$_T$BioMAT Graduate Training for Rationally Designed, Integrative Biomaterials (T32 EB 006343), U.S. DOE GAANN award, the Georgia Tech Center for Drug Design, Development and Delivery, and the Georgia Tech TI:GER program. Funding for SS was provided by the NSF Integrative Graduate Education and Research Traineeship program in Stem Cell Biomanufacturing (0965945). Funding for DEM was provided by the NSF REU Program.

■ REFERENCES

(1) (a) Caruso, F. *Adv. Mater.* **2001**, *13*, 11. (b) Glotzer, S. C.; Solomon, M. J. *Nat. Mater.* **2007**, *6*, 557. (c) Buck, M. R.; Bondi, J. F.; Schaak, R. E. *Nature Chem.* **2012**, *4*, 37.

(2) (a) Peyratout, C. S.; Dahne, L. *Angew. Chem., Int. Ed.* **2004**, *43*, 3762. (b) Johnston, A. P. R.; Such, G. K.; Ng, S. L.; Caruso, F. *Curr. Opin. Colloid Interface Sci.* **2011**, *16*, 171. (c) Yan, Y.; Such, G. K.; Johnston, A. P. R.; Lomas, H.; Caruso, F. *ACS Nano* **2011**, *5*, 4252.

(3) (a) Lu, Y.; Mei, Y.; Drechsler, M.; Ballauff, M. *Angew. Chem., Int. Ed.* **2006**, *45*, 813. (b) Mei, Y.; Lu, Y.; Polzer, F.; Ballauff, M.; Drechsler, M. *Chem. Mater.* **2007**, *19*, 1062.

(4) (a) Caruso, F.; Caruso, R. A.; Möhwald, H. *Science* **1998**, *282*, 1111. (b) Okubo, M.; Lu, Y.; Wang, Z. *Colloid Polym. Sci.* **1999**, *277*, 77. (c) Li, H.; Han, J.; Panioukhine, A.; Kumacheva, E. *J. Colloid Interface Sci.* **2002**, *255*, 119. (d) Chen, R.; Pearce, D. J. G.; Fortuna, S.; Cheung, D. L.; Bon, S. A. F. *J. Am. Chem. Soc.* **2011**, *133*, 2151.

(5) (a) Vincent, B.; Young, C. A.; Tadros, T. F. *Faraday Discuss.* **1978**, *65*, 296. (b) Furusawa, K.; Anzai, C. *Colloids Surf.* **1992**, *63*, 103. (c) Harley, S.; Thompson, D. W.; Vincent, B. *Colloids Surf.* **1992**, *62*, 163.

(6) (a) Li, R.; Yang, X. L.; Li, G. L.; Li, S. N.; Huang, W. Q. *Langmuir* **2006**, *22*, 8127. (b) Fleming, M. S.; Mandal, T. K.; Walt, D. R. *Chem. Mater.* **2001**, *13*, 2210.

(7) (a) Ming, W.; Wu, D.; van Benthem, R.; de With, G. *Nano Lett.* **2005**, *5*, 2298. (b) Tsai, H. J.; Lee, Y. L. *Langmuir* **2007**, *23*, 12687.

(8) (a) Nayak, S.; Lyon, L. A. *Angew. Chem., Int. Ed.* **2005**, *44*, 7686. (b) Kabanov, A. V.; Vinogradov, S. V. *Angew. Chem., Int. Ed.* **2009**, *48*, 5418.

(9) Pelton, R. *Adv. Colloid Interface Sci.* **2000**, *85*, 1.

(10) (a) Hoare, T.; Pelton, R. *Langmuir* **2004**, *20*, 2123. (b) Xu, J. J.; Timmons, A. B.; Pelton, R. *Colloid Polym. Sci.* **2004**, *282*, 256.

(11) (a) Islam, A. M.; Chowdhry, B. Z.; Snowden, M. J. *J. Phys. Chem.* **1995**, *99*, 14205. (b) Atkin, R.; Bradley, M.; Vincent, B. *Soft Matter* **2005**, *1*, 160. (c) Agrawal, M.; Rubio-Retama, J.; Zafeiropoulos, N. E.; Gaponik, N.; Gupta, S.; Cimrova, V.; Lesnyak, V.; Lopez-Cabarcos, E.; Tzavalas, S.; Rojas-Reyna, R.; Eychmuller, A.; Stamm, M. *Langmuir* **2008**, *24*, 9820.

(12) (a) Mrkic, J.; Saunders, B. R. *J. Colloid Interface Sci.* **2000**, *222*, 75. (b) Kim, J.-W.; Fernandez-Nieves, A.; Dan, N.; Utada, A. S.; Marquez, M.; Weitz, D. A. *Nano Lett.* **2007**, *7*, 2876. (c) Dechezelles, J. F.; Malik, V.; Crassous, J. J.; Schurtenberger, P. *Soft Matter* **2013**, *9*, 2798.

(13) Bridges, A. W.; Singh, N.; Burns, K. L.; Babensee, J. E.; Lyon, L. A.; Garcia, A. J. *Biomaterials* **2008**, *29*, 4605.

(14) (a) Nolan, C. M.; Serpe, M. J.; Lyon, L. A. *Biomacromolecules* **2004**, *5*, 1940. (b) Serpe, M. J.; Yarmey, K. A.; Nolan, C. M.; Lyon, L. A. *Biomacromolecules* **2005**, *6*, 408.

(15) (a) Lyon, L. A.; Debord, J. D.; Debord, S. B.; Jones, C. D.; McGrath, J. G.; Serpe, M. J. *J. Phys. Chem. B* **2004**, *108*, 19099. (b) Iyer, A. S.; Lyon, L. A. *Angew. Chem., Int. Ed.* **2009**, *48*, 4562. (c) Meng, Z.; Cho, J. K.; Breedveld, V.; Lyon, L. A. *J. Phys. Chem. B* **2009**, *113*, 4590.

(16) Debord, J. D.; Eustis, S.; Debord, S. B.; Lofye, M. T.; Lyon, L. A. *Adv. Mater.* **2002**, *14*, 658.

(17) Hermanson, G. T. *Bioconjugate Techniques*; Academic Press: San Diego, CA, 1996.

(18) Singh, N.; Bridges, A. W.; Garcia, A. J.; Lyon, L. A. *Biomacromolecules* **2007**, *8*, 3271.